27th Conf. on Weather Analysis and Forecasting/
23nd Conf. on Numerical Weather Prediction.
AMS, Chicago, IL, June 28 - July 3, 2015.

32 AN OVERVIEW OF CAPS STORM-SCALE ENSEMBLE FORECAST FOR THE 2015 NOAA HWT SPRING FORECASTING EXPERIMENT

Fanyou Kong[1]*, Ming Xue[1,2], Youngsun Jung[1], Keith A. Brewster[1],
Kevin W. Thomas[1], Yunheng Wang[1], Feifei Shen[1],
Israel L. Jirak[3], Adam Clark[4], J. Correia Jr.[3], Steven J. Weiss[3], Michael C. Coniglio[4], C. J. Melick[3]
[1]Center for Analysis and Prediction of Storms, and [2]School of Meteorology,
University of Oklahoma, Norman, OK 73072
[3]NOAA/NMS/NCEP Storm Prediction Center
[4]NOAA National Severe Storm Laboratory, Norman, OK 73072

1. INTRODUCTION

The Center for Analysis and Prediction of Storms (CAPS) at the University of Oklahoma produces realtime storm-scale ensemble forecast (SSEF) each spring season since 2007 to support the NOAA Hazardous Weather Testbed (HWT) Spring Forecast Experiment(Kong et al. 2007; 2008; 2009; 2012; 2014a,b; Xue et al. 2007; 2008; 2009; 2010). The 2015 CAPS SSEF realtime forecast ran from April 20 to June 5, 2015, using WRF-ARW with a domain covering the full continental United States (CONUS) with convection-allowing resolution at 3-km horizontal grid spacing. CAPS SSEF members were configured with a hybrid of initial/lateral boundary condition (IC/LBC) perturbations extracted from the operational NCEP Short-Range Ensemble Forecast (SREF) ensemble members (at 16 km grid spacing) and various combinations of physics options in microphysics, PBL and land-surface model. Up to 140 WSR-88D Doppler weather radar data over the CONUS, with both radial wind and reflectivity, and other observation data were analyzed into the SSEF members in realtime using the ARPS 3DVAR and Complex Cloud Analysis system (Gao et al. 2004; Hu et al. 2006). An experimental EnKF-based ensemble was also produced from a one hour EnKF cycles at 15 min interval from 2300 to 0000 UTC with all available radar and other observation data.

This extended abstract first provides highlights to the CAPS SSEF for 2015 HWT Spring Forecast Experiment in Section 2, followed by quantitative verification results on QPF in Section 3. The comparison of EnKF-based ensemble and 3DVAR initiated ensemble has been presented in Section 4.

2. EXPERIMENT HIGHLIGHT

The CAPS 2015 Storm-Scale Ensemble Forecast (SSEF) started on 20 April through 5 June 2015, encompassing the NOAA HWT 2015 Spring Forecast Experiment that is officially between 4 May and 5 June. Different from past years, the 2015 SSEF CONUS domain is changed from 4-km to 3-km horizontal grid spacing, resulting in 2.1 times more grid points and covering 18% more area than in the 2014 season (Figure 1). The migration to a 3-km grid spacing makes CAPS SSEF more consistent with the operational HRRR setting. As in previous years, the forecasts are produced Monday through Friday, initialized at 0000 UTC (1900 CDT) each day and made available in early morning for evaluation at HWT.

There are two suites of SSEF runs. One is the ordinary 0000 UTC 3-km ensembles consist of 20 WRF-ARW members (Table 1) initialized with a onetime 3DVAR analysis, with the forecast lead time of 60 hours. The ensemble is configured with a combination of IC/LBC perturbations and physics variations. For the perturbed members, 3-hourly forecasts from consistent NCEP SREF members were used to provide the lateral boundary conditions. The second suite is a newly implemented realtime EnKF based forecasting that includes a one hour EnKF cycling DA at 15 min interval from 2300 UTC to 0000 UTC following a 5-h 40-member ensemble forecast initiated from 1800 UTC, over the same CONUS domain as the ordinary SSEF.

In order to provide an ensemble background for EnKF, a separate 3-km ensemble of 5-h forecasts, starting at 1800 UTC, with 40 WRF-ARW members is produced over the same CONUS domain. This ensemble is configured with initial perturbations and mixed physics options to provide input for EnKF analysis. Each member uses WSM6 microphysics with different parameter settings in rain and graupel number concentration and graupel density (Table 2). No radar data is analyzed for this set of runs. All members also include random perturbations with recursive filtering of ~20 km horizontal correlations scales, with relatively small perturbations (0.5K for potential temperature and 5% for relative humidity). EnKF analysis (cycling), with radar data and other conventional data, is performed from 2300 to 0000 UTC every 15 min, using as background the 40-member ensemble. A 11-member ensemble forecast (60h) follows using the 0000 UTC EnKF analyses (Table 3). In addition, four deterministic forecasts, two (one with Thompson and another with WSM6 microphysics) from the ensemble mean analysis and another two (Thompson, WSM6) from 3DVAR cycling, are also produced. Ensemble products from both suites are available to HWT participants in the morning.

WRF-ARW V3.6.1 was used, with different microphysics and PBL schemes assigned for different members. In addition to Thompson, Milbrandt-Yau, and Morrison microphysics schemes, two newly developed P3 (Predicted Particle Properties) microphysics by Morrison and Milbrandt (Personal communications), one with a single ice category and another with two ice

**Corresponding Author Address*: Dr. Fanyou Kong, Center for Analysis and Prediction of Storms, Univ. of Oklahoma, Norman, OK 73072; E-mail: *fkong@ou.edu*

categories, are implemented and included in 2015 SSEF. A Thompson scheme addressing fractional cloudiness is also included. Model simulated radar reflectivity is computed within each individual microphysics algorithm. PBL schemes used include MYJ, MYNN, and a modified YSU by Greg Thompson in an attempt to correct the overly dry and warm PBL issue of YSU.

Tables 1 lists member configurations for the 3DVAR initialized SSEF ensemble. *cn* refers to the control member, with radar data analysis, *c0* is the same as *cn* except for no radar data was analyzed in. *m3* – *m13* are members with both IC/LBC perturbation and physics variations, while *cn*, *c0*, and *m14* – *m20* are members without IC and LBC perturbation but only physics variations. NAMa and NAMf refer to the 12 km NAM analysis and forecast, respectively. ARPSa refers to analysis after ARPS 3DVAR and Cloud Analysis using NAMa as the background. Table 2 lists member configurations for the 40 member EnKF background ensemble initiated at 1800 UTC; while Table 3 lists configurations for the 0000 UTC EnKF-based ensemble.

The 3DVAR initiated SSEF forecasts were performed on *Stampede*, a Dell C8220 supercomputer system with over 6400 Intel Xeon Phi computing nodes at TACC at the University of Texas at Austin, utilizing 950 computing nodes each day in the overnight hours. The EnKF ensemble forecasts were performed on *Darter*, a Cray XC30 supercomputer system with 12,000 computing cores, at the NSF sponsored National Institute of Computational Sciences (NICS) at the University of Tennessee. Hourly model outputs were archived on the mass storages on Ranch at TACC and HPSS at NICS.

A total of 33 days of complete ensemble forecasts from the 0000 UTC 3DVAR initialized SSEF runs were produced during the experiment period. Using the NSSL 1-km resolution Multi-Radar/Multi-Sensor (MRMS) QPE data (Zhang et al. 2011) as a verification dataset, the SSEF QPF and probabilistic QPF performance has been evaluated using various traditional verification metrics.

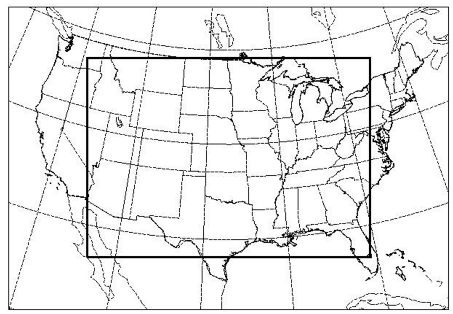

Figure 1. Model forecast domains for the 2015 Season (1680×1152, at 3-km grid spacing). The small inner domain (1080x760) is the QPF verification region.

*Table 1. Configurations for ARW members. NAMa and NAMf refer to the 12 km NAM analysis and forecast, respectively. ARPSa refers to ARPS 3DVAR and cloud analysis**

Member	IC	BC	Radar data	Microphysics	LSM	PBL
arw_cn	00Z ARPSa	00Z NAMf	yes	Thompson	Noah	MYJ
arw_c0	00Z ARPSa	00Z NAMf	no	Thompson	Noah	MYJ
arw_m3	arw_cn + nmmb-p2_pert	21Z SREF nmmb-p2	yes	P3	Noah	MYNN
arw_m4	arw_cn + nmmb-n2_pert	21Z SREF nmmb-n2	yes	M-Y	Noah	YSU
arw_m5	arw_cn + nmm-p1_pert	21Z SREF nmm-p1	yes	Morrison	Noah	MYNN
arw_m6	arw_cn + nmmb-n1_pert	21Z SREF nmmb-n1	yes	M-Y	Noah	MYJ
arw_m7	arw_cn + nmmb-p1_pert	21Z SREF nmmb-p1	yes	P3	Noah	YSU
arw_m8	arw_cn + em-n1_pert	21Z SREF em-n1	yes	P3	Noah	MYJ
arw_m9	arw_cn + em-p2_pert	21Z SREF em-p2	yes	M-Y	Noah	MYNN
arw_m10	arw_cn + nmmb-n3_pert	21Z SREF nmmb-n3	yes	Morrison	Noah	YSU
arw_m11	arw_cn + nmmb-p3_pert	21Z SREF nmmb-p3	yes	Thompson	Noah	YSU
arw_m12	arw_cn + nmm-n3_pert	21Z SREF nmm-n3	yes	Thompson	Noah	MYNN

arw_m13	arw_cn + nmm-p2_pert	21Z SREF nmm-p2	yes	Morrison	Noah	MYJ
arw_m14	00Z ARPSa	00Z NAMf	yes	Thompson	Noah	MYNN
arw_m15	00Z ARPSa	00Z NAMf	yes	Thompson	Noah	YSU-T
arw_m16	00Z ARPSa	00Z NAMf	yes	Thompson ICLOUD=3	Noah	YSU-T
arw_m17	00Z ARPSa	00Z NAMf	yes	MY	Noah	MYJ
arw_m18	00Z ARPSa	00Z NAMf	yes	P3-cat2	Noah	MYJ
arw_m19	00Z ARPSa	00Z NAMf	yes	P3	Noah	MYJ
arw_m20	00Z ARPSa	00Z NAMf	yes	Morrison	Noah	MYJ

* *For all members: ra_lw_physics= RRTMG; ra_sw_physics=RRTMG; cu_physics= NONE. Member m25 uses Thompson modified RRTMG in coupled mode for both sw and lw radiations. Member arw_m16 accounts for sub-grid scale clouds in the RRTMG radiation scheme based on research by G. Thompson. Arw_m18 uses the newly developed P3 (Morrison-Milbrandt) microphysics with two-category ice; all other P3 members are with one-category ice.*

Table 2. Configuration for the 1800 UTC EnKF ensembles

Member	IC	BC	Microphysics – WSM6* (N0r, N0g, ρg)	LSM	PBL
enk_m1	18Z NAMa	18Z NAMf	(8,6),(4,6),500	Noah	MYJ
enk_m2	enk_m1 + em-p1_pert	15Z SREF em-p1	(8,6),(4,6),500	Noah	YSU
enk_m3	enk_m1 + nmm-n2_pert	15Z SREF nmm-n2	(9.4,6),(5,4),673	Noah	MYJ
enk_m4	enk_m1 + em-n2_pert	15Z SREF em-n2	(2.4,7),(5.7,4),666	Noah	ACM2
enk_m5	enk_m1 + nmmb-p2_pert	15Z SREF nmmb-p2	(3.7,7),(6.3,4),659	Noah	ACM2
enk_m6	enk_m1 + nmm-p1_pert	15Z SREF nmm-p1	(2.5,6),(8,4),652	Noah	MYNN
enk_m7	enk_m1 + nmmb-n1_pert	15Z SREF nmmb-n1	(2.6,7),(9,4),645	Noah	MYJ
enk_m8	enk_m1 + nmmb-p1_pert	15Z SREF nmmb-p1	(6.8,6),(1,5),638	Noah	YSU
enk_m9	enk_m1 + em-n1_pert	15Z SREF em-n1	(3,6),(1.1,5),631	Noah	MYJ
enk_m10	enk_m1 + em-p2_pert	15Z SREF em-p2	(8.4,6),(1.3,5),624	Noah	MYNN
enk_m11	enk_m1 + nmmb-n3_pert	15Z SREF nmmb-n3	(1.5,7),(1.4,5),617	Noah	MYJ
enk_m12	enk_m1 + nmmb-p3_pert	15Z SREF nmmb-p3	(3.1,6),(1.6,5),610	Noah	YSU
enk_m13	enk_m1 + em-p3_pert	15Z SREF em-p3	(8.6,5),(1.8,5),603	Noah	ACM2
enk_m14	enk_m1 + nmm-p2_pert	15Z SREF nmm-p2	(4.6,6),(2,5),596	Noah	MYNN
enk_m15	enk_m1 + em-p1_pert	15Z SREF em-p1	(1.3,7),(2.2,5),589	Noah	MYNN
enk_m16	enk_m1 + nmm-n2_pert	15Z SREF nmm-n2	(5.1,6),(2.5,5),582	Noah	ACM2
enk_m17	enk_m1 + em-n2_pert	15Z SREF em-n2	(8.1,5),(2.8,5),575	Noah	MYJ

enk_m18	enk_m1 + nmmb-p2_pert	15Z SREF nmmb-p2	(1.9,6),(3.2,5),568	Noah	ACM2
enk_m19	enk_m1 + nmm-p1_pert	15Z SREF nmm-p1	(3.9,7),(3.6,5),561	Noah	MYJ
enk_m20	enk_m1 + nmmb-n1_pert	15Z SREF nmmb-n1	(2.2,6),(4,5),554	Noah	ACM2
enk_m21	enk_m1 + nmmb-p1_pert	15Z SREF nmmb-p1	(8.5,6),(4.5,5),547	Noah	MYJ
enk_m22	enk_m1 + em-n1_pert	15Z SREF em-n1	(1.1,7),(5,5),540	Noah	MYJ
enk_m23	enk_m1 + em-p2_pert	15Z SREF em-p2	(8.1,5),(5.7,5),533	Noah	YSU
enk_m24	enk_m1 + nmmb-n3_pert	15Z SREF nmmb-n3	(1,7),(6.4,5),526	Noah	MYNN
enk_m25	enk_m1 + nmmb-p3_pert	15Z SREF nmmb-p3	(2.2,7),(7.1,5),519	Noah	MYNN
enk_m26	enk_m1 + em-p3_pert	15Z SREF em-p3	(7.2,6),(8,5),512	Noah	MYJ
enk_m27	enk_m1 + nmm-p2_pert	15Z SREF nmm-p2	(8.9,6),(9,5),505	Noah	YSU
enk_m28	enk_m1 + nmmb-p3_pert	15Z SREF nmmb-p3	(2.9,7),(1,6),498	Noah	ACM2
enk_m29	enk_m1 + em-p3_pert	15Z SREF em-p3	(1.1,7),(1.1,6),491	Noah	MYNN
enk_m30	enk_m1 + nmm-p2_pert	15Z SREF nmm-p2	(9.6,6),(1.3,6),484	Noah	MYJ
enk_m31	enk_m1 + em-p1_pert	15Z SREF em-p1	(3.1,6),(1.4,6),477	Noah	YSU
enk_m32	enk_m1 + nmm-n2_pert	15Z SREF nmm-n2	(1.3,6),(1.6,6),470	Noah	MYNN
enk_m33	enk_m1 + em-n2_pert	15Z SREF em-n2	(2,6),(1.8,6),463	Noah	MYJ
enk_m34	enk_m1 + nmmb-p2_pert	15Z SREF nmmb-p2	(4.4,6),(2,6),456	Noah	YSU
enk_m35	enk_m1 + nmm-p1_pert	15Z SREF nmm-p1	(1.7,6),(2.2,6),449	Noah	ACM2
enk_m36	enk_m1 + nmmb-n1_pert	15Z SREF nmmb-n1	(4.3,6),(2.5,6),442	Noah	MYNN
enk_m37	enk_m1 + nmmb-p1_pert	15Z SREF nmmb-p1	(1.3,6),(2.8,6),435	Noah	MYNN
enk_m38	enk_m1 + em-n1_pert	15Z SREF em-n1	(9.1,5),(3.2,6),428	Noah	MYJ
enk_m39	enk_m1 + em-p2_pert	15Z SREF em-p2	(5,6),(3.6,6),421	Noah	YSU
enk_m40	enk_m1 + nmmb-n3_pert	15Z SREF nmmb-n3	(6.1,6),(3.9,6),414	Noah	MYJ

** For N0r and N0h, (a, b) are coefficients of $a \times 10^b$.*

Table 3. Configuration for the EnKF-based 0000 UTC ensemble forecasts

Member	IC	BC	Microphysics	LSM	PBL
enkf_cn	enk_m1a	00Z NAMf	Thompson	Noah	MYJ
enkf_m6	enk_m2a	21Z SREF nmmb-n1	M-Y	Noah	MYJ
enkf_m9	enk_m6a	21Z SREF em-p2	M-Y	Noah	MYNN

enkf_m10	enk_m8a	21Z SREF nmmb-n3	Morrison	Noah	YSU
enkf_m5	enk_m10a	21Z SREF nmm-p1	Morrison	Noah	MYNN
enkf_m4	enk_m12a	21Z SREF nmmb-n2	M-Y	Noah	YSU
enkf_m3	enk_m17a	21Z SREF nmmb-p2	P3	Noah	MYNN
enkf_m8	enk_m23a	21Z SREF em-n1	P3	Noah	MYJ
enkf_m7	enk_m26a	21Z SREF nmmb-p1	P3	Noah	YSU
enkf_m12	enk_m37a	21Z SREF nmm-n3	Thompson	Noah	MYNN
enkf_m11	enk_m39a	21Z SREF nmmb-p3	Thompson	Noah	YSU
enkf_mn_thom	enfamean_thom	00Z NAMf	Thompson	Noah	MYJ
enkf_mn_wsm6	enfamean_wsm6	00Z NAMf	WSM6	Noah	MYJ
enkf_3dvar_thom	3dvar_thom	00Z NAMf	Thompson	Noah	MYJ
enkf_3dvar_wsm6	3dvar_wsm6	00Z NAMf	WSM6	Noah	MYJ

3. QPF VERIFICATION

3.1 Deterministic QPF

The 3DVAR initiated SSEF members, their ensemble mean and the probability matched mean (PM) are evaluated in terms of QPF against the MRMS QPE (Zhang et al. 2011). The 1-km resolution QPE data are remapped to the 3-km model verification sub-domain (see in Figure 1) that has edges off the coasts and outside CONUS trimmed off. Equitable threat scores (ETS) and other traditional metrics are calculated over the verification sub-domain and averaged over 33 complete forecast dates.

Figures 2 and 3 are the ETS plots for the 1-h and 3-h accumulated precipitation, respectively. The initially higher scores reflect the benefit of radar data assimilation. This beneficial effect drops quickly as forecast proceeds. Low scores are seen over the convection active afternoon and evening hours. Overall, PM scores the highest compared with individual members and with ensemble mean excepting for the light rain threshold of 1-h accumulated precipitation in Figure 2a. PM outscores ensemble mean especially in heavier rain thresholds.

3.2 Deterministic QPF in neighborhood context

Traditional verification metrics tend to penalize location errors, even for small misplacement of rain bands. It is not uncommon, on the other hand, for SSEF members on the convection-allowing grid spacing to predict overall good but misplaced convection systems. Human forecasters can have certain tolerance level in interpreting high-resolution NWP QPF. Taking into such considerations, ETS scores are recalculated with a neighborhood context by searching ±r grid points in each direction. Taking grid (i,j) and r=2 as an example, a condition is met if any grid point from i-2 to i+2 and from j-2 to j+2 meets the set condition.

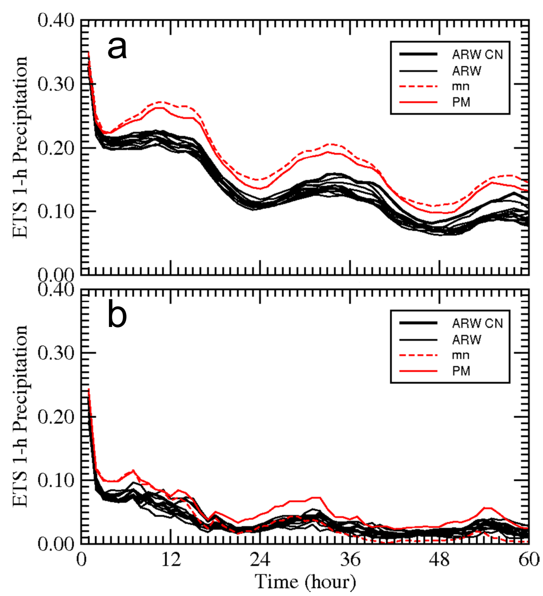

Figure 2. ETS of 1-h accumulated precipitation (a) ≥0.01 inch and (b) ≥0.25 inch, averaged over 33 dates over the verification domain.

Figure 4 shows the ETS scores of 3-h accumulated precipitation for ensemble PM with r=0, 2, 4. With increasing level of special tolerance level (value r), the ETS increases. With a 12 km (r=4) tolerance level, the initial ETS doubles for the light rain threshold and triples for the 0.5 inch threshold.

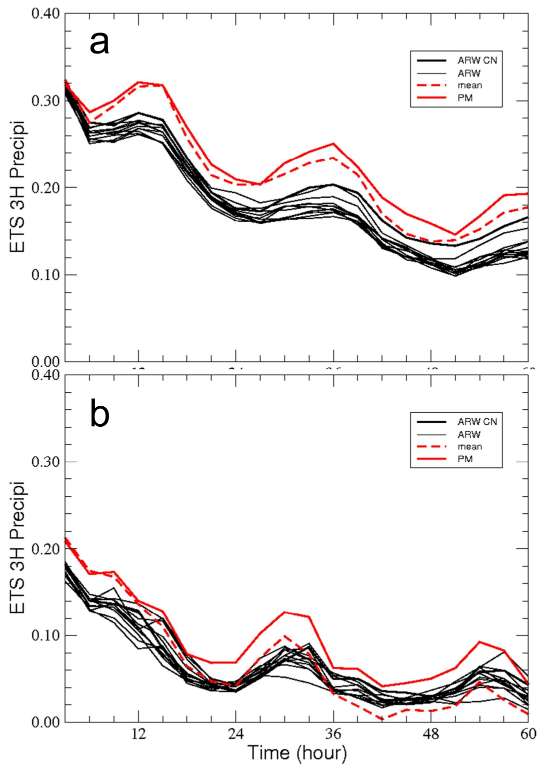

Figure 3. ETS of 3-h accumulated precipitation (a) ≥0.01 inch and (b) ≥0.5 inch, averaged over 33 dates over the verification domain.

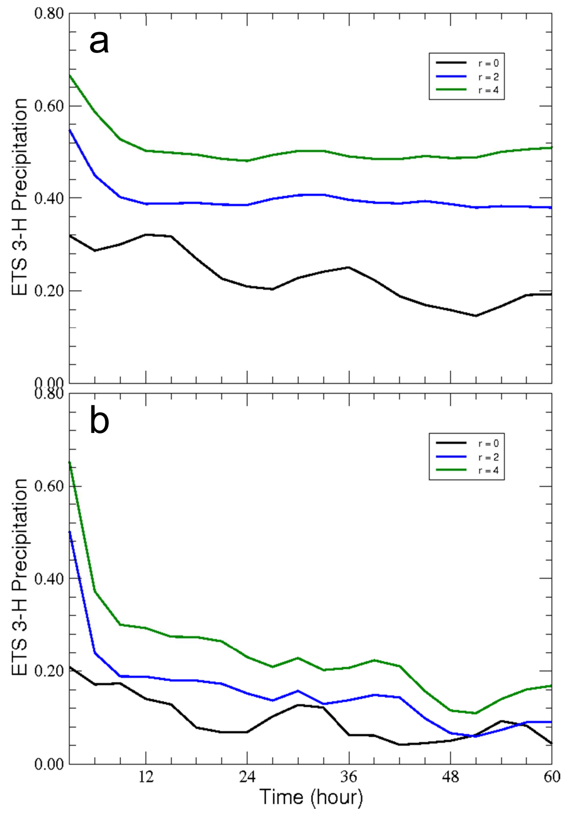

Figure 4. ETS of the probability matched mean (PM) 3-h accumulated precipitation (a) ≥0.01 inch and (b) ≥0.5 inch, averaged over 33 dates over the verification domain, with various radius in the neighborhood context.

3.3 Probabilistic QPF

The Relative Operating Characteristic (ROC) curves at 24 h forecast lead time are plotted for the ensemble probability of 3-h accumulated precipitation ≥ 0.5 inch in Figure 5. The closer an ROC curve is toward the upper left corner, the better the probability forecast is. An ROC curve is termed 'worthless' if it sits on the diagonal line connecting the points (0,0) and (1,1). The area under ROC curve (AUROC) provides a quantitative measure of the worthiness of the probabilistic forecast. An AUROC of 1 represents a perfect forecast and 0.5 represents a worthless forecast. The four ROC curves in Figure 5 have AUROC values of 0.716, 0.799, 0.828, 0.850, respectively, with r ranging from 0 to 13, indicating fair to good forecast accuracy.

Figure 6 plots the AUROC curves with three QPF thresholds, throughout the 60 h forecast duration. Without employing neighborhood context (r=0), it shows that the PQPF for the thresholds 0.25 and 0.5 inch have AUROC values larger than 0.7 during most of the 60 h forecast duration; while for the 1.0 inch threshold the AUROC values fall below 0.7 beyond 12 h.

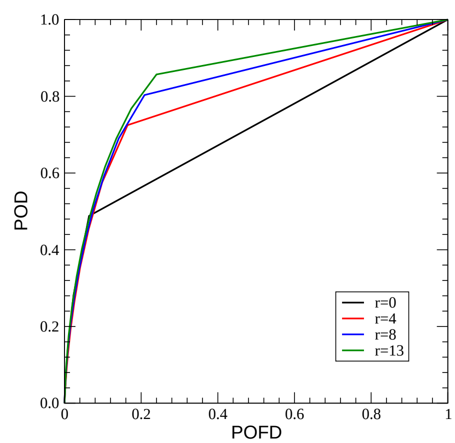

Figure 5. ROC curves for the ensemble probability of 3-h accumulated precipitation ≥ 0.5 inch at 24 h forecast lead time, with different neighborhood tolerant levels.

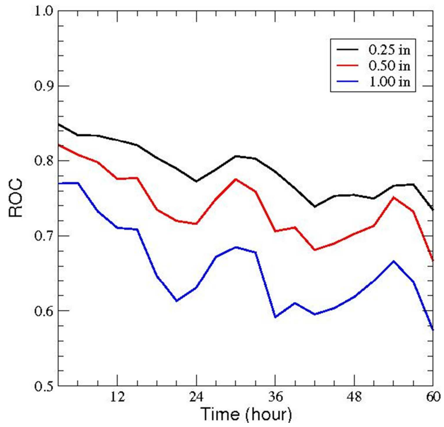

Figure 6. AUROCs for the ensemble probability of 3-h accumulated precipitation≥0.25, 0.5, and 1.0 inch with r=0.

Figure 7 shows the reliability diagram for the 24 h forecast time for the probabilistic QPF (PQPF) of 3-h accumulated precipitation ≥0.5 inch. Along with the point-to-point curve (r=0), three reliability lines are show with different neighborhood tolerant levels ranging from 12 km (r=4) to 40 km (r=13). It can be seen that with point-to-point verification, the PQPF is significantly over-forecasted. Increasing neighborhood tolerant level does reduce the degree of over-forecast. With r=4, there is under-forecast in low probability and over-forecast in higher probability. With r=13, it is under-forecast overall.

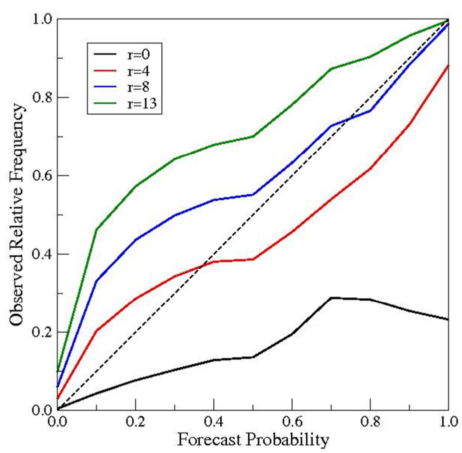

Figure 7. Reliability diagram for the 24 h forecast hour PQPF of 3-h accumulated precipitation ≥0.5 inch.

4. ENKF VS 3DVAR IN SSEF

The ETS scores of the EnKF-based ensemble forecasts starting at 0000 UTC are evaluated, along with its ensemble mean and PM, and four deterministic runs initiated using the EnKF mean and cycled 3DVAR analysis. There are 25 dates of mostly complete runs.

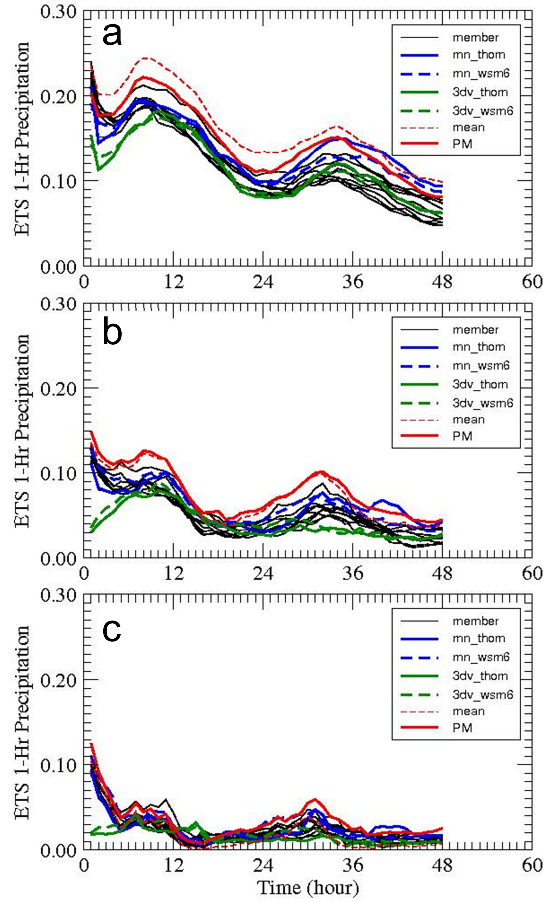

Figure 8. ETS of 1-h accumulated precipitation (a) ≥0.01, (b) ≥0.10, (c) ≥0.25 inch, from the EnKF-based 0000 UTC ensemble members, mean, PM, and four deterministic forecasts.

Figure 8 plots the ETS scores of 1-h accumulated precipitation averaged over 25 days. Only the values up to 48 h are drawn since there are incomplete data beyond 48 h in some dates. Between the two sets of deterministic forecasts, those initiated from EnKF mean (blue lines) outperform those from cycled 3DVAR, esp. in the early forecast hours. It is true that the EnKF-based ensemble, driven from 1800 UTC NAM background, scores lower in terms of QPF compared with the onetime 3DVAR initiated SSEF that is driven from 0000 UTC NAM background. More effort will be dedicated in the future studies to refining the EnKF system to optimize its performance in convection allowing NWP framework.

Acknowledgements

This project is mainly funded by a grant from the NOAA Collaborative Science, Technology, and Applied Research (CSTAR) program (NA10NWS4680001), with other supports from the NSF and NOAA. All storm-scale ensemble forecasting runs were performed on Stampede in TACC at the University of Texas at Austin and on Darter in the National Institute of Computational Sciences (NICS) at the University of Tennessee as part of the national XSEDE supercomputing allocation, part of post processing tasks were performed on Boomer in the Oklahoma Supercomputer Center for Education and Research (OSCER) at the University of Oklahoma.

5. REFERENCES

Gao, J.-D., M. Xue, K. Brewster, and K. K. Droegemeier, 2004: A three-dimensional variational data analysis method with recursive filter for Doppler radars. *J. Atmos. Ocean. Tech.*, **21,** 457-469.

Hu, M., M. Xue, J. Gao, and K. Brewster, 2006: 3DVAR and cloud analysis with WSR-88D level-II data for the prediction of Fort Worth tornadic thunderstorms. Part II: Impact of radial velocity analysis via 3DVAR. *Mon. Wea. Rev.*, **134,** 699-721.

Jung, Y., G. Zhang, and M. Xue, 2008: Assimilation of simulated polarimetric radar data for a convective storm using ensemble Kalman filter. Part I: Observation operators for reflectivity and polarimetric variables. *Mon. Wea. Rev.*, **136,** 2228-2245.

Jung, Y., M. Xue, and G. Zhang, 2010: Simulations of polarimetric radar signatures of a supercell storm using a two-moment bulk microphysics scheme. *J. Appl. Meteor. Climatol.*, **49,** 146-163.

Jung, Y., M. Xue, Y. Wang, S. Wang, F. Kong, Y. Pan, and K. Zhu, 2013: Multi-Scale Ensemble Kalman Filter Data Assimilation and Forecasts in Central United States. *WMO 6th Symposium on Data Assimilation*.

Kong, F., and Coauthors, 2007: Preliminary analysis on the real-time storm-scale ensemble forecasts produced as a part of the NOAA hazardous weather testbed 2007 spring experiment. *22nd Conf. Wea. Anal. Forecasting/18th Conf. Num. Wea. Pred.*, Salt Lake City, Utah, Amer. Meteor. Soc., CDROM 3B.2.

Kong, F., and Coauthors, 2008: Real-time storm-scale ensemble forecast experiment - Analysis of 2008 spring experiment data. *24th Conf. Several Local Storms*, Savannah, GA, Ameri. Meteor. Soc., Paper 12.13.

Kong, F., and Coauthors, 2009: A real-time storm-scale ensemble forecast system: 2009 Spring Experiment. *23nd Conf. Wea. Anal. Forecasting/19th Conf. Num. Wea. Pred.*, Omaha, Nebraska, Amer. Meteor. Soc., Paper 16A.13.

Kong, F., and Coauthors, 2012: CAPS Storm-Scale Ensemble Forecasts for the NOAA 2012 HWT Spring Experiment: New Features and QPF Verification. *13th WRF Users Workshop*, Paper 5.3.

Kong, Fanyou, and Coauthors, 2014a: CAPS Storm-Scale Ensemble Forecasting System: Impact of IC and LBC perturbations. 26th WAF/22nd NWP Conf, AMS, Atlanta GA, Paper 119.

Kong, Fanyou, and Coauthors, 2014b: An Overview of CAPS Storm-Scale Ensemble Forecast for the 2014 NOAA HWT Spring Forecasting Experiment. 27th Conference on Severe Local Storms, AMS, Madison WI, Paper 43.

Xue, M., and Coauthors, 2007: CAPS realtime storm-scale ensemble and high-resolution forecasts as part of the NOAA Hazardous Weather Testbed 2007 spring experiment. *22nd Conf. Wea. Anal. Forecasting/18th Conf. Num. Wea. Pred.*, Amer. Meteor. Soc., CDROM 3B.1.

Xue, M., and Coauthors, 2008: CAPS realtime storm-scale ensemble and high-resolution forecasts as part of the NOAA Hazardous Weather Testbed 2008 Spring Experiment. *24th Conf. Several Local Storms*, Savannah, GA, Ameri. Meteor. Soc., Paper 12.12.

Xue, M., and Coauthors, 2009: CAPS realtime multi-model convection-allowing ensemble and 1-km convection-resolving forecasts for the NOAA Hazardous Weather Testbed 2009 Spring Experiment. *23nd Conf. Wea. Anal. Forecasting/19th Conf. Num. Wea. Pred.*, Omaha, NB, Amer. Meteor. Soc., Paper 16A.12.

Xue, M., and Coauthors, 2010: CAPS Realtime Storm Scale Ensemble and High Resolution Forecasts for the NOAA Hazardous Weather Testbed 2010 Spring Experiment. *25th Conf. on Severe Local Storms*, Amer. Meteor. Soc., 7B.3.

Zhang, J., and Coauthors, 2011: National Mosaic and Multi-Sensor QPE (NMQ) System: Description, Results, and Future Plans. *Bulletin of the American Meteorological Society*, **92,** 1321-1338.